Steady and Unsteady Transonic Airloads on a Supercritical Wing

S. Y. Ruo* and J. B. Malone*
Lockheed-Georgia Company, Marietta, Georgia
and
J. J. Horsten† and R. Houwink‡
National Aerospace Laboratory (NLR), Amsterdam, The Netherlands

A brief description of an experimental investigation to determine steady and unsteady airloads on a fixed and an oscillating supercritical wing model is presented. Steady and unsteady data are correlated with results of computational methods for various representative cases. Steady transonic flow computations were carried out using the XTRAN3S code and the Bailey-Ballhaus/McNally code. Unsteady flow computations were performed using the XTRAN3S code and a quasi-three-dimensional method, which combines the LTRAN2-NLR code with subsonic theory. Compared to the experimental data, the computed results show qualitatively similar transonic effects on pressure distributions and lift coefficients. The accuracy, however, is only modest.

Nomenclature

B	= semi-span (1.0 m)
B – B	= Bailey-Ballhaus steady wing code
B – B/M	= Bailey-Ballhaus code coupled with McNally plane boundary-layer code
c	= local chord
c_{AC}	= mean aerodynamic chord (0.268 m)
C_m	= sectional moment coefficient about local quarter chord
C_M	= wing moment coefficient about aerodynamic center, X_{AC}
C_p	= pressure coefficient
C_z	= sectional normal force coefficient
C_Z	= wing normal force coefficient
f	= frequency, Hz
i	$=\sqrt{-1}$
k	= reduced frequency $= \pi f c_{AC}/U_\infty$
M_∞	= freestream Mach number
$Q-3-D$	= quasi-three-dimensional method of NLR
U_∞	= freestream velocity
X	= chordwise ordinate
X_{AC}	= aerodynamic center (0.291 m)
XTRAN3S	= transonic steady and unsteady wing code
Y	= spanwise ordinate
α_m	= mean angle of attack, deg
$\Delta\alpha$	= angular amplitude of displacement transducer or angular increment for quasi-steady calculation, deg
θ	= cyclic angular position, deg

Superscripts

$(\ )'$	= real part
$(\ )''$	= imaginary part
$(\ )^*$	= critical condition

Subscript

1	= first harmonic

Presented as Paper 83-1686 at the AIAA 16th Fluid and Plasma Dynamics Conference, Danvers, Mass., July 12-14, 1983; received Dec. 1, 1983; revision received Aug. 8, 1984.

*Scientist.
†Research Engineer.
‡Senior Research Engineer.

Introduction

THE availability of accurate computational aerodynamics methods is important to the successful development of reliable aeroelastic prediction techniques. In the past decade, the availability of larger, high-speed computers and advances in computational fluid dynamics have led to the development of improved numerical aerodynamic analysis procedures. Unfortunately, experimental data suitable for code correlation efforts, especially unsteady data, are scarce, and are virtually nonexistent for advanced-technology wings at transonic speeds.

To meet this need, a cooperative program was initiated in 1979 to produce a transonic aerodynamic data base for both steady and unsteady flows on an aft-loaded transport aircraft wing. This program resulted in the acquisition of experimental data validating new computational methods and providing insight into three-dimensional unsteady transonic flow phenomena. This wing model, known as LANN wing, for Lockheed-Georgia, Air Force Wright Aeronautical Laboratories, NASA Langley, and the National Aerospace Laboratory (NLR) of the Netherlands, has been designated as one of the five AGARD three-dimensional standard aeroelastic configurations.[1]

The results of the experimental investigation are presented in Ref. 2. Correlations of theoretical and experimental results are reported in Refs. 3 and 4. This paper summarizes the experimental and theoretical investigations, and concentrates on the correlation of results for a number of representative cases.

Experiment

LANN Model Description

The LANN model wing (Fig. 1) shape is similar to that of the supercritical Wing A model, previously developed and investigated by Hinson and Burdges.[5] The model wing has a simple planform (Fig. 1). Its geometry is obtained by linear interpolation between the supercritical airfoil sections at the root and tip. The materials chosen for the model were suitable for a cryogenic test environment. The model has an aspect ratio of 7.92, thickness ratio of 0.12, 1.0-m semi-span and 0.361-m root chord. The sweep angles of the leading edge, trailing edge, and 0.25 chord line are 27.5, 16.9, and 25.0 deg, respectively. The model was fitted with transition strips at a distance of 5% of the mean aerodynamic chord downstream of the wing leading edge.

The LANN model was instrumented to measure surface pressures in order to provide a data base which could be used

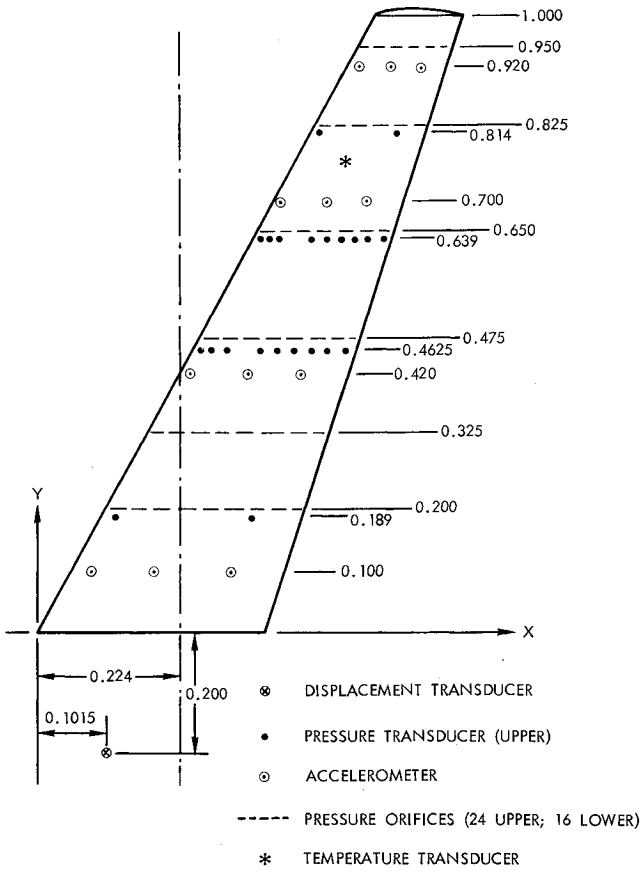

Fig. 1 LANN wing geometry and instrumentation.

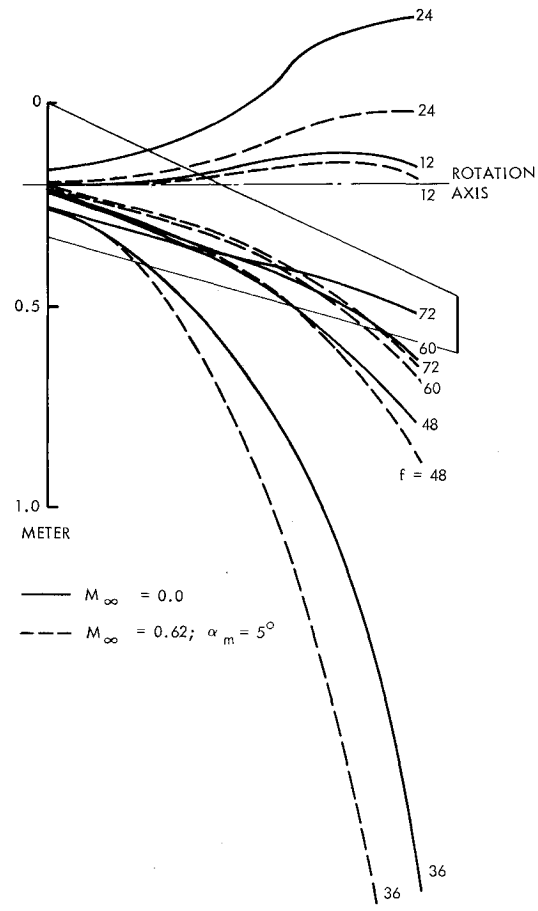

Fig. 2 Influence of Mach number on nodal line position.

to verify transonic-flow computer codes. A total of 212 pressure orifices were positioned in chordwise rows at six wing span stations. The spanwise locations of the pressure orifice rows are shown in Fig. 1. At four wing span stations, a total of 22 in-situ pressure transducers were mounted near orifice rows. These transducers were used in the NLR measuring technique (summarized below) to determine tube transfer functions for the unsteady pressures measured through the static pressure orifices.

During unsteady testing, the model aeroelastic mode shape was measured using 12 accelerometers and one linear variable differential transformer (LVDT). The LVDT was positioned near the wing root station and was used to monitor the amplitude and mean steady incidence of the motion input to the model. The accelerometers were located in chordwise rows at 4 wing span stations. The placement of these accelerometers on the wing planform is shown in Fig. 1.

Test Facility

Tests of the LANN wing model were performed in the transonic wind tunnel (HST) of NLR (Ref. 2). This is a closed-circuit wind tunnel with a test section of 1.6×2.0 m and a velocity range of $M_\infty = 0.0$ to $M_\infty = 1.28$. Typical Reynolds numbers of 5×10^6 based on mean aerodynamic chord were attained on the model during testing.

The wing model was attached to a support that was mounted on a turntable at the sidewall of the tunnel test section. The mean angle of attack of the model could be adjusted remotely over a ± 3 deg range with respect to the support angle. The angle of the support, in turn, was adjusted by rotating the turntable.

The wing pitch oscillation about an axis normal to the wind tunnel sidewall was introduced by a hydraulic activator. The amplitude of oscillation could be adjusted up to 1.0 deg, while the frequency could be varied between 0 and 72 Hz. Due to the model natural frequency of about 30 Hz, the unsteady aeroelastic mode shape was strongly dependent on the frequency. The influence of frequency and flow conditions on the nodal line location is shown in Fig. 2.

Data reduction was carried out using PHAROS (Processor for Harmonic Analysis of the Response of Oscillating Surfaces), NLR's data acquisition and reduction system. Output quantities from the PHAROS system are the zeroth (steady component) and the real and imaginary components of the first harmonic of the unsteady pressures. In addition, higher harmonic contributions can be obtained when required. Sectional lift and moment coefficients are also obtained by integration of surface pressure distributions.

Measuring Technique

Surface pressure measurements on the LANN model were made using the NLR measurement technique (Refs. 6 and 7). This method is particularly well suited to handle a large amount of pressure data at a relatively low cost. This technique involves using conventional static pressure tube/scanning valve instrumentation for dynamic as well as static measurements. For unsteady flow cases, the tube geometry, mean velocity level, and frequency of the pressure fluctuation play a significant role in the dynamic response of the measuring system. To determine the necessary tube response corrections, the actual transfer functions of selected reference tubes were measured with 22 in-situ pressure transducers. The measured transfer functions were then used to calibrate the remaining pressure tube responses.

Accuracy

It is generally recognized that it is extremely difficult to quantify the accuracy of measured unsteady aerodynamic data. At attached transonic flow conditions a rough estimate of the accuracy of unsteady pressure measurements for the LANN model is about 5% in magnitude and 3 deg in phase angle.

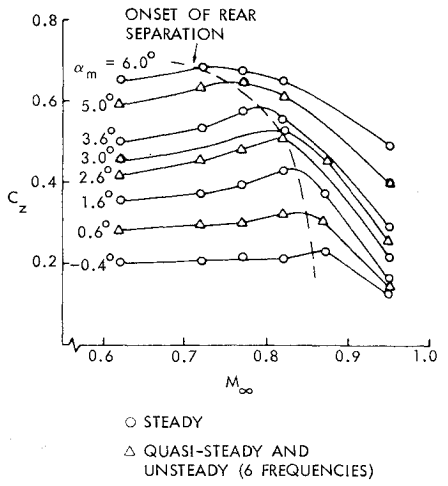

Fig. 3 Test conditions of LANN wing model.

The accuracy of lift and moment coefficients depends in particular upon the spacing of pressure orifices in regions with large pressure gradients. In some wing sections of the LANN model, at shock waves and in the outboard nose region, the spacing was not sufficiently dense to obtain an accurate description of the local pressure peaks. As a result the measured airloads are less accurate than the measured pressures, and probably are slightly lower than in reality. For a theory-experiment correlation, the measured pressure distributions should be preferred as a basis for comparison.

The experimental results are not corrected for wall interference effects. Steady results may be corrected using the following estimated correction to the angle of attack:

$$\Delta\alpha = a_l C_Z \text{ deg}$$

where a_l varies linearly from -0.25 at $M_\infty = 0.5$ to -0.5 at $M_\infty = 0.8$. The effect of this correction on the quasi-steady lift C_{l_α}/π is an increase of approximately 2 to 5%. This gives an indication of the magnitude of wall interference effects on the unsteady airloads.

Test Conditions

Figure 3 summarizes the combinations of Mach number, incidence and lift coefficient at which steady and unsteady measurements have been taken for the LANN model. The majority of unsteady tests were taken at an amplitude of 0.25 deg, at frequencies varying from 12 to 72 Hz. At a limited number of conditions the effect of amplitude (up to 1 deg) and the presence of higher harmonics was measured. For a complete description of the test program and results, see Ref. 2. In the present paper a limited number of cases are used for correlation with various computational methods, discussed in the next sections.

Computational Methods

The three transonic flow numerical methods used for comparison with the selected portion of the LANN wing data base were 1) the XTRAN3S unsteady small disturbance wing code (Ref. 8), 2) a Bailey-Ballhaus steady small disturbance wing code (Ref. 9) coupled with the McNally plane boundary-layer code (Ref. 10), and 3) a quasi-three-dimensional (Q-3-D) method using LTRAN2-NLR, an unsteady transonic small disturbance airfoil code, and subsonic three-dimensional corrections (Ref. 11).

The XTRAN3S Code

The version of the XTRAN3S code used in this study includes the improved spanwise grid distribution and the partial vectorization of the program provided by NASA Langley. This code uses a time-dependent small disturbance equation and an alternating direction implicit algorithm originally developed by Borland and Rizetta (Ref. 8). The tangency condition on the wing is satisfied in a mean chord plane. The initial condition for the calculation is an undisturbed uniform flow. A restart from previously calculated results is possible. This feature facilitates the continuation of any calculation for which converged results are not yet achieved. The computed results are considered to have converged when all the transients have disappeared from the computational flow field.

The Bailey-Ballhaus/McNally Code

The B-B/M code is a code that weakly couples the viscous effect, i.e., McNally code, with the Bailey-Ballhaus steady wing code by employing the surface transpiration velocity to simulate two-dimensional boundary-layer effects. Since the flow in the spanwise direction on a transport type aircraft wing is usually seen to be small, this weak coupling scheme seems to be reasonable. This code, like most other viscous codes, is limited to unseparated flows for reliable results. Although the calculations may be continued after flow separation, the numerical results thus obtained, however, must be used with caution. The tangency, initial and convergence conditions used in B-B/M code are similar to those used in the XTRAN3S code.

The NLR Quasi-Three-Dimensional (Q-3-D) Method

The computational method for three-dimensional unsteady transonic flow used at NLR is an engineering method which combines two-dimensional transonic theory with two- and three-dimensional subsonic linear theory.[11] An early version of this method was reported in Ref. 12. Applications to the LANN model are reported in Ref. 4.

The method was applied as follows for the harmonically oscillating model with given steady-state pressure distributions. Using the LTRAN2-NLR code,[13] unsteady transonic airloads were computed for one representative wing section ($Y/B = 0.475$) in unit pitch and heave motions at various values of mean incidence and frequency. The theoretical incidence was adjusted in advance to obtain approximate matching of theoretical and experimental shock wave location. Subsequently, distributions of two-dimensional airloads over the wing span were obtained by interpolation in the above set of results, taking into account the sectional reduced frequency and local lift coefficient. As a basis for three-dimensional correction procedure, subsonic theory was used to compute two- and three-dimensional unsteady aerodynamic influence coefficients. The final distributions of unsteady airloads was obtained by combination of the two-dimensional transonic results with the two- and three-dimensional subsonic results for the actual vibration mode. A subsonic three-dimensional correction was also applied to the computed two-dimensional unsteady transonic pressure distribution at the representative wing section.

In addition to the inviscid results, viscous effects were computed for a few cases using the LTRAN2-NLR code coupled with Green's lag-entrainment method (LTRANV code).[14]

Steady Results

The numerical results of the XTRAN3S code presented in this section were obtained using the program options of the modified form of the small disturbance equations together with NLR coefficients. Low- and high-frequency options, respectively, were used for the steady and unsteady flow calculations. The boundary conditions were steady downstream, unsteady wake, and unsteady lifting surface for unsteady flow and all steady conditions for the steady flow calculations. The computational mesh used was 13-span-station by 39-chordwise-point on the half-wing. The slope at

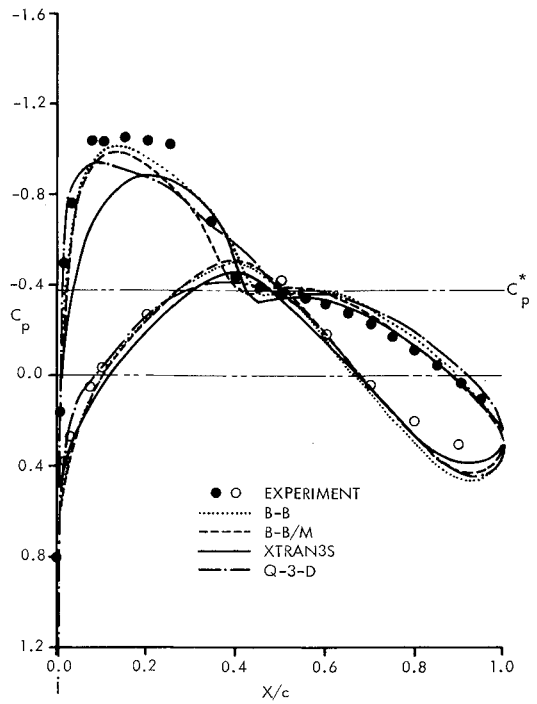

Fig. 4 Steady pressure coefficients for $M_\infty = 0.82$, $\alpha_m = 0.6$ at $Y/B = 0.475$.

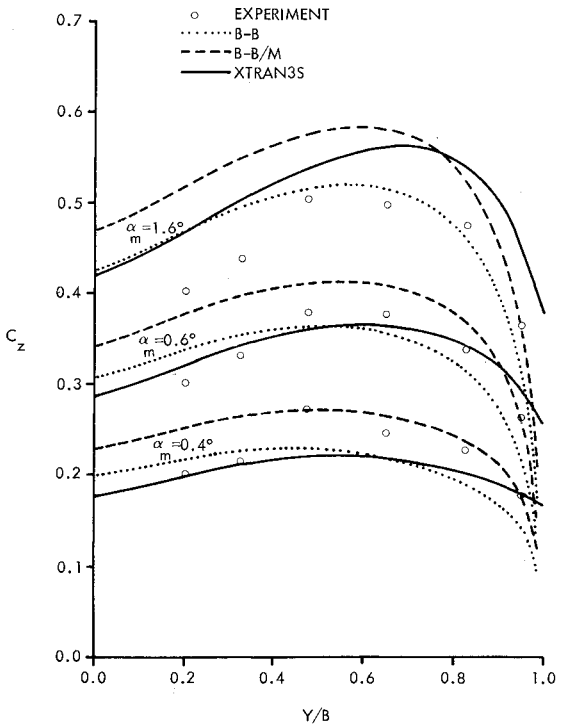

Fig. 5 Steady spanwise normal force distributions at different angles of attack for $M_\infty = 0.82$.

the computational mesh points was interpolated from eight fitted polynomials for the measured wing ordinates.

The numerical results of B-B/M code presented here were obtained with the full conservative option of the code. The computational mesh used was 25-span-station by 49-chordwise-point on the half-wing. The wing ordinates at the grid points of XTRAN3S, i.e., the output of XTRAN3S code, were used as input for the B-B/M code to maintain consistency in wing geometry.

Shown in Fig. 4 are the typical steady inviscid flow results near mid semi-span (47.5%) obtained from XTRAN3S, B-B/M, and Q-3-D and the measured data for a freestream Mach number of 0.82 and a mean angle of attack of 0.60 deg. All numerical methods underpredicted the leading edge suction peak and the shock strength at all span stations calculated. This may be due to the lack of mesh points near these flow regions where the gradients are high. Also, the numerical results showed more rear loading than experimentally observed. This compensates for the deficit in the predicted normal force on the wing ahead of the shock. Therefore, the normal force always correlates better with the experimental data than the moment coefficient does. The comparison of the calculated results with the measured data is generally better for the inboard sections than for the outboard sections.[3] The results obtained from the viscid option of the B-B/M code also are included in this figure. The viscous effect reduces the level of leading edge suction from the inviscid results and shifts the shock location quite noticeably even though the flow is still attached. For Q-3-D results, in spite of the matching of theoretical and experimental shock wave location, differences still exist at the rear half of the airfoil and in the supersonic flow region.

The span loading distribution at three angles of attack at 0.82 Mach number is shown in Fig. 5. The agreement between the experimental and theoretical results is better at a smaller than at a higher angle of attack. That span loading distribution of XTRAN3S at the wing tip does not approach zero as fast as the experimental and the other theoretical results is probably due to the lack of mesh points used. The results from the viscid option of the B-B/M code seem to correlate fairly well with the measured data.

The integrated wing normal force and moment about the aerodynamic center at several angles of attack for a fixed Mach number is shown in Figs. 6 and 7. The slope of normal force with respect to angle of attack at a fixed Mach number is quite linear at small angle of attack. The agreement with the measured data is very good for the XTRAN3S and the viscid B-B/M codes. Even though the experimentally observed flow separation did not take place until the angle of attack was greater than 2.9 deg, the theoretical method started to fail at 2.0 deg.

Unsteady Results

The correlation of unsteady flow results is given in this section. The theoretical results were that of XTRAN3S, B-B/M codes, and the Q-3-D method. Only the results of one frequency, 24 Hz, are presented in detail. The zero frequency case was approximated from the results of steady flow calculations. The effects of frequency and Mach number on airloads are also shown.

Unsteady pressure coefficients are presented in the following form:

$$C_{pi} = C_p' + iC_p'' = C_{pI}/\Delta\alpha \tag{1}$$

Unsteady airloads are obtained by integration of the unsteady pressure distributions. Sectional airloads coefficients are presented as follows:

lift

$$C_{zi} = C_z' + iC_z'' = \frac{1}{\pi} C_{zI}\Big/\Delta\alpha \tag{2}$$

moment (positive nose down, about 1/4 chord)

$$C_{mi} = C_m' + iC_m'' = \frac{1}{\pi} C_{mI}\Big/\Delta\alpha \tag{3}$$

A similar notation is used for the wing unsteady lift and moment coefficients C_{Zi} and C_{Mi}. The reference length for

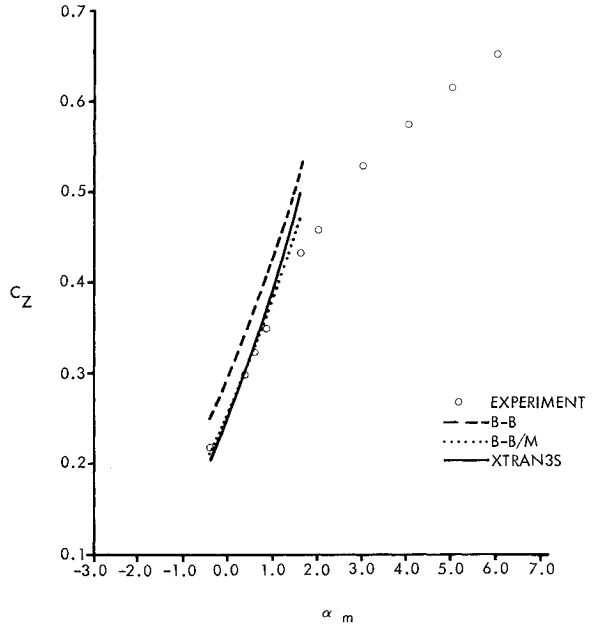

Fig. 6 Steady wing normal force vs mean angle of attack for $M_\infty = 0.82$.

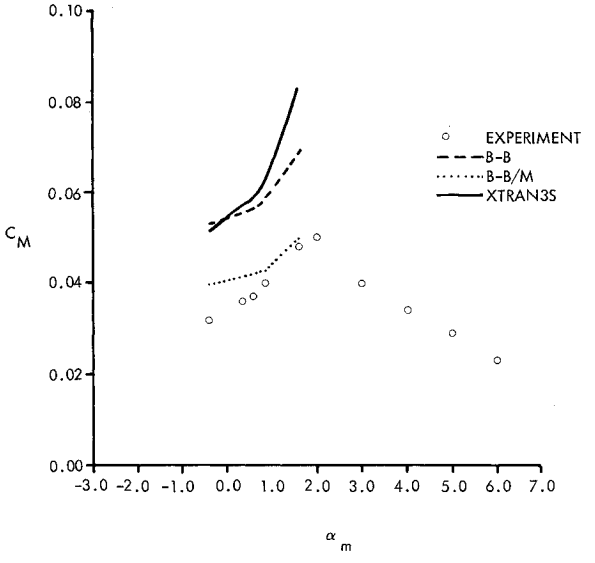

Fig. 7 Steady wing moment coefficient vs mean angle of attack for $M_\infty = 0.82$.

C_{Mi} is the mean aerodynamic chord and is determined about an axis through the mean aerodynamic chord quarter-chord point normal to the wind tunnel sidewall.

For zero frequency (quasi-steady results) the first harmonic components in Eqs. (1) to (3) were determined in an approximate manner using steady results at incidences $\alpha_m + \Delta\alpha$ and $\alpha_m - \Delta\alpha$, for instance:

$$C_{pl} = [C_p(\alpha_m + \Delta\alpha) - C_p(\alpha_m - \Delta\alpha)]/(2\Delta\alpha)$$

Quasi-steady lift and moment coefficients were determined analogously.

Quasi-Steady

The quasi-steady result obtained for a 0.82 Mach number and 0.60 deg mean angle of attack perturbed by 0.25 deg is shown in Figs. 8, 9, and 10. In Fig. 8, the calculated pressure along a near mid-semi-span station from XTRAN3S, Q-3-D,

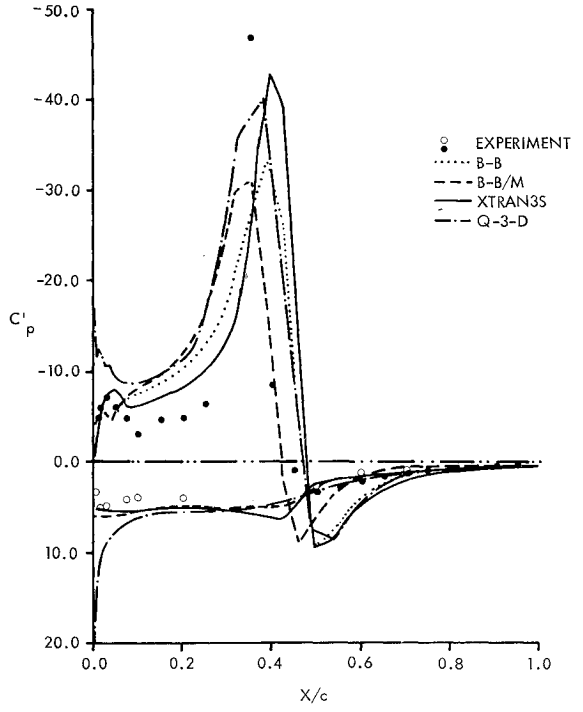

Fig. 8 Quasi-steady pressure coefficients for $M_\infty = 0.82$, $\alpha_m = 0.6$ at $Y/B = 0.475$.

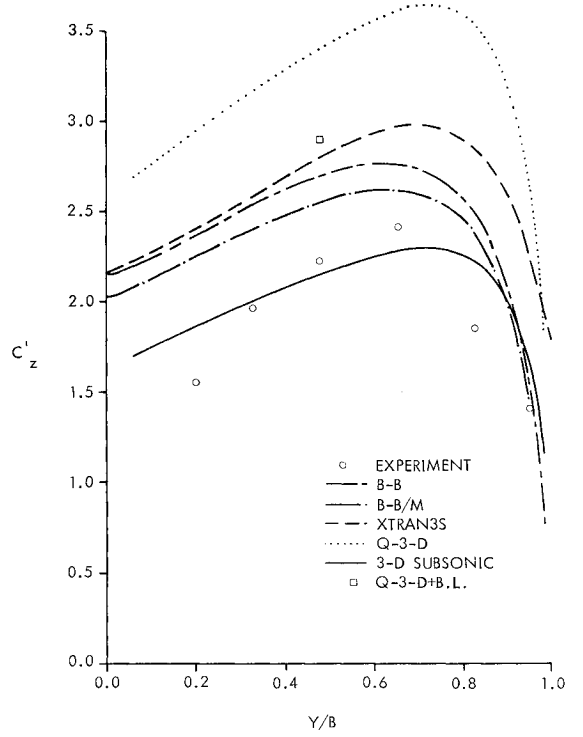

Fig. 9 Quasi-steady spanwise normal force distribution for $M_\infty = 0.82$, $\alpha_m = 0.60$, and $\Delta\alpha = 0.25$.

and both inviscid and viscid options from B-B/M are shown, while the sectional lift and moment coefficients are shown in Figs. 9 and 10. All numerical results overpredicted the quasi-steady upper surface pressure and underpredicted the shock shift due to the perturbation of the mean angle of attack along the inboard sections. Overprediction near wing tip by XTRAN3S code is far more than the B-B/M code.

The quasi-steady sectional lift and moment coefficients (Figs. 9 and 10) show a general overprediction of C_z', especially the results of Q-3-D method and a reasonable prediction of C_m'. The large overprediction of C_z' with Q-3-

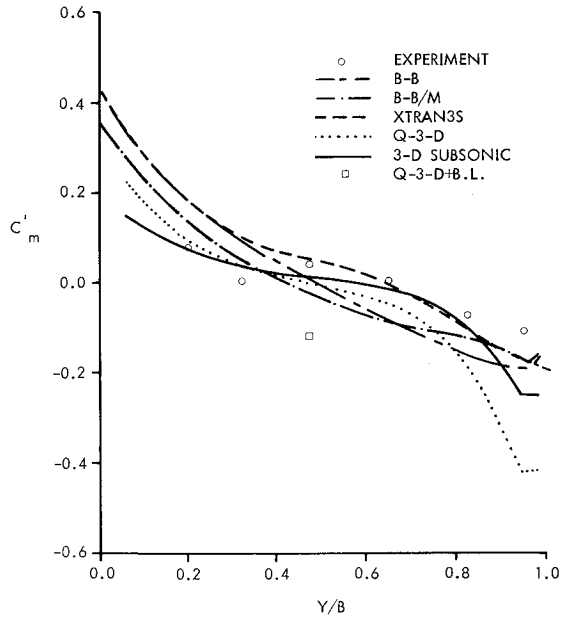

Fig. 10 Quasi-steady spanwise moment coefficient distributions for $M_\infty = 0.82$, $\alpha_m = 0.60$, and $\Delta\alpha = 0.25$.

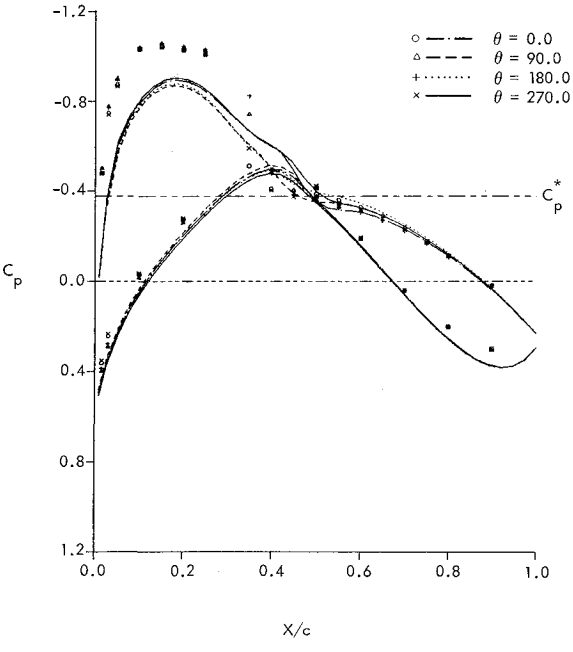

Fig. 11 Chordwise pressure distributions at various pitch angular positions for $M_\infty = 0.82$, $\alpha_m = 0.6$, $\Delta\alpha = 0.25$, and $f = 24$ Hz at $Y/B = 0.475$.

D, which is caused by accounting for transonic effects, is stronger than that by the either XTRAN3S or B – B code shown in Fig. 9. Apparently the subsonic three-dimensional effect implied in the Q-3-D method does not give a sufficient reduction of the transonic sectional lift coefficients. Surprisingly, the subsonic theory shows the best agreement with the experimental results. In general, the inclusion of viscous effect has shown improvement on the lift coefficient from the inviscid results. Viscous results for a near mid-semi-span station, obtained using the LTRANV code with the Q-3-D method, show an improvement. For unknown reasons, however, this viscous correction, obtained using Green's lag-entrainment method, is much stronger than the viscous correction computed in the B-B/M code using the boundary layer method of McNally.

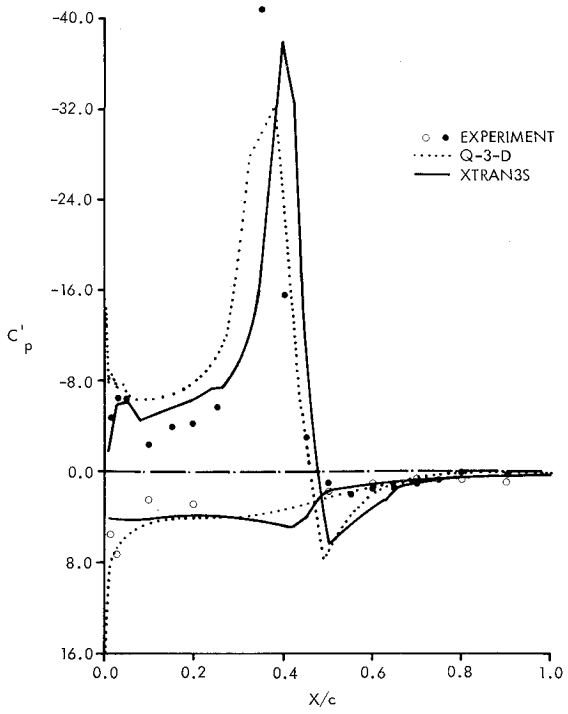

Fig. 12a Unsteady pressure coefficients for $M_\infty = 0.82$, $\alpha_m = 0.6$, $\Delta\alpha = 0.25$, and $f = 24$ Hz at $Y/B = 0.475$, real.

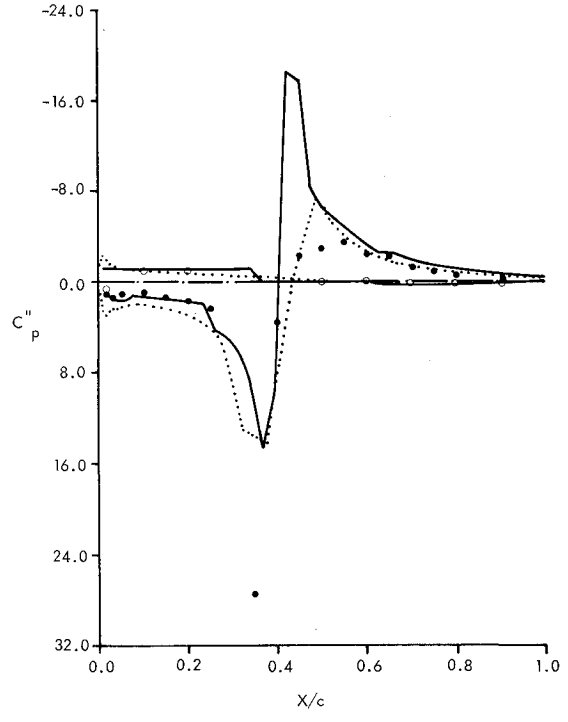

Fig. 12b Unsteady pressure coefficients for $M_\infty = 0.82$, $\alpha_m = 0.6$, $\Delta\alpha = 0.25$, and $f = 24$ Hz at $Y/B = 0.475$, imaginary.

Unsteady

The unsteady flow calculations were made for a Mach number of 0.82, a mean angle of attack of 0.6 deg, and a pitching amplitude of 0.25 deg at 24 Hz (a reduced frequency of 0.076 based on the mean aerodynamic chord). The results are shown in Figs. 11 to 14. A comparison between the XTRAN3S and the measured chordwise pressure along mid semi-span station at different angular positions is shown in Fig. 11. The fluctuation of pressure over the wing during one cycle of pitch oscillation is rather small, except near the shock. The calculated results showed a larger shock excursion

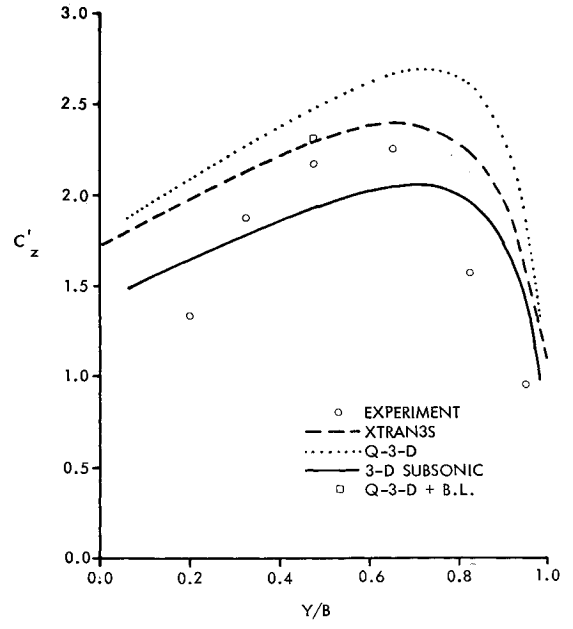

Fig. 13a Unsteady spanwise normal force distributions for $M_\infty = 0.82$, $\alpha_m = 0.6$, $\Delta\alpha = 0.25$, and $f = 24$ Hz, real.

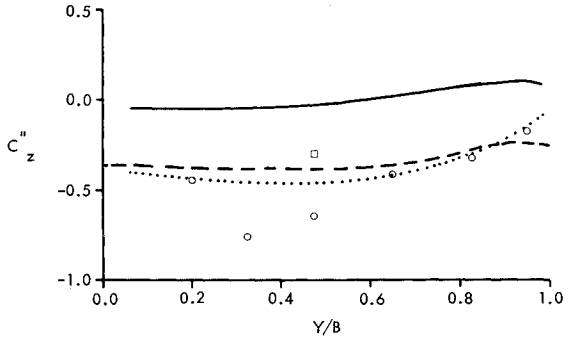

Fig. 13b Unsteady spanwise normal force distributions for $M_\infty = 0.82$, $\alpha_m = 0.6$, $\Delta\alpha = 0.25$, and $f = 24$ Hz, imaginary.

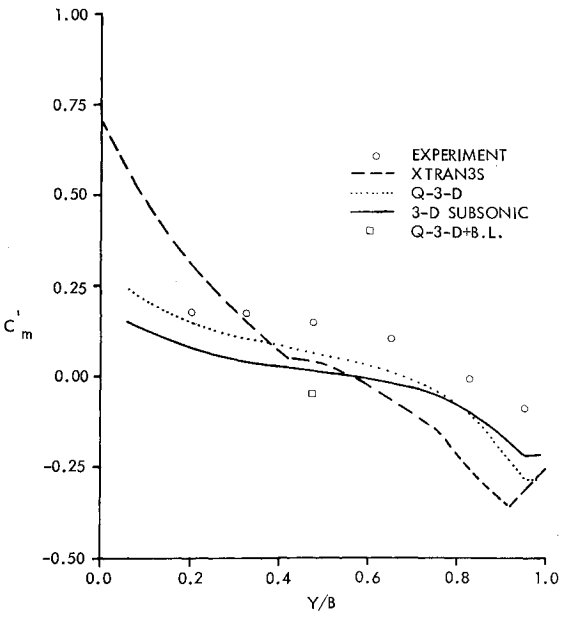

Fig. 14a Unsteady spanwise moment coefficient distributions for $M_\infty = 0.82$, $\alpha_m = 0.60$, $\Delta\alpha = 0.25$, and $f = 24$ Hz, real.

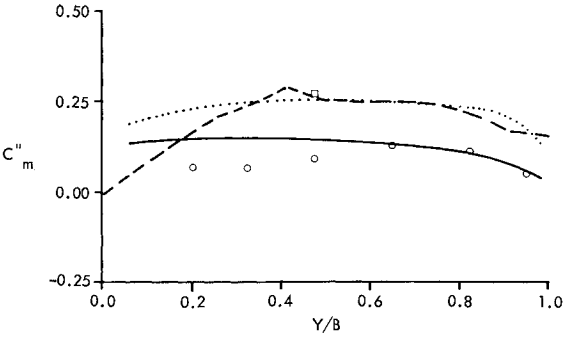

Fig. 14b Unsteady spanwise moment coefficient distributions for $M_\infty = 0.82$, $\alpha_m = 0.60$, $\Delta\alpha = 0.25$, and $f = 24$ Hz, imaginary.

in terms of the local chord near the tip rather than near the root. It is rather difficult to see clearly the exact shock excursion from the experimental data because of the spacing of the measuring orifices. From the available experimental data, however, it is observed that the shock movement seems to be larger near the mid-semi-span than either the tip or the root.

The computed unsteady pressure distributions (Fig. 12) of XTRAN3S and Q-3-D for the near mid-span station show a similar comparison with the experimental results as in the quasi-steady case. Due to the prior matching of the steady pressure distribution, the location of the unsteady pressure peaks of Q-3-D agrees well with the experimental result. The results of XTRAN3S are quite reasonable, except the predicted pressure peak of the real part is slightly downstream of the experimental data.

The unsteady sectional lift distributions are shown in Fig. 13. Both real and imaginary parts of XTRAN3S results again compared well with the experimental data. The real part of three-dimensional subsonic method agrees well with the experimental data but not the imaginary part. Accounting for transonic effects in Q-3-D yields an overprediction of C_z', but it improves the prediction of C_z'' considerably. The unsteady moment coefficients (Fig. 14), are not predicted accurately. The transonic effects in Q-3-D caused an increase in the magnitude of both C_z and C_m by approximately 30% and a decrease in phase angle by approximately 10 deg and 10%, respectively, for C_z and C_m. To investigate the effect of viscosity, results of the LTRANV code for a near mid-span station were combined with the Q-3-D method. Accounting for the boundary layer, as in the quasi-steady case, only improves the prediction of C_z'.

Frequency Effect

The effect of frequency on the unsteady airloads is investigated for $f = 0$, 24, and 48 Hz at $M_\infty = 0.82$ and $\alpha_m = 0.6$ deg with $\Delta\alpha = 0.25$ deg.

A global impression of the effect of frequency on the unsteady airloads is given in Fig. 15, which shows the unsteady lift and moment coefficients of the wing. Here it should be noted that the vibration mode also varies with frequency, which causes a discontinuity in C_l and C_M near the frequency of about 30 Hz ($k = 0.09$), which corresponds to the natural first bending mode of the model. Like the sectional coefficients, C_l' is overpredicted, whereas C_l'' is reasonably well predicted by both XTRAN3S and Q-3-D method. At $f = 0$ and 24 Hz, the Q-3-D method predicts a similar, but somewhat stronger, transonic effect on C_l than the XTRAN3S code. The unsteady moment coefficients, again, are not predicted accurately by any method.

The transonic effects included in Q-3-D tend to increase the magnitude of both C_l and C_M, but decrease the phase angle from its three-dimensional subsonic theory counterpart. Both magnitude and phase angle decrease as the frequency increases except the magnitude of C_M increases as frequency increases from zero then decreases as the frequency increases further.

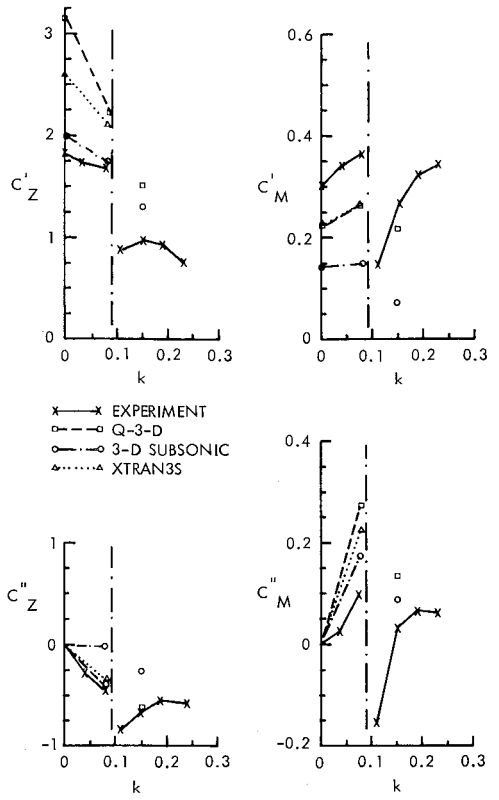

Fig. 15 Effects of frequency on wing lift and moment coefficients for $M_\infty = 0.82$, $\alpha_m = 0.6$, and $\Delta\alpha = 0.25$.

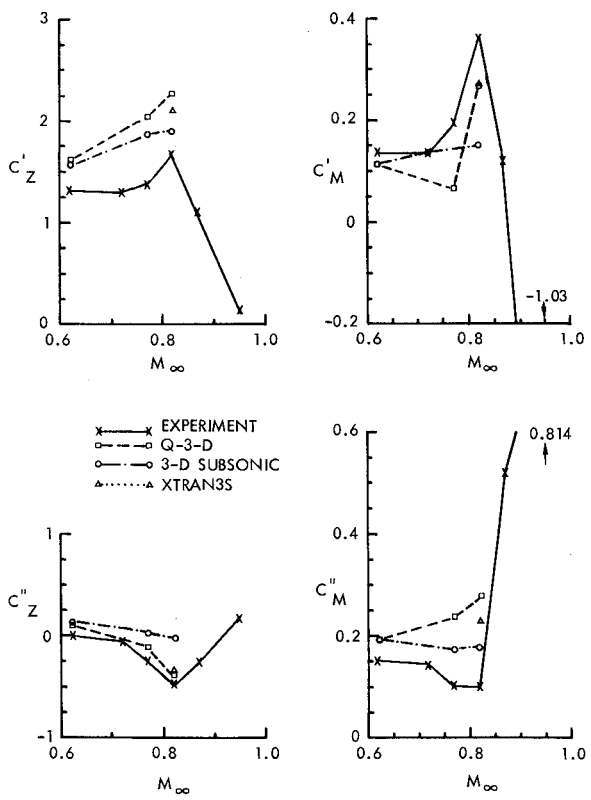

Fig. 16 Effects of Mach number on wing lift and moment coefficients for $\alpha_m = 0.6$, $\Delta\alpha = 0.25$, and $f = 24$ Hz.

Mach Number Effect

To investigate the effect of Mach number on the unsteady airloads for $\alpha_m = 0.6$ deg and f = 24 Hz, the Q-3-D method was applied at $M_\infty = 0.6$ and 0.77 in addition to 0.82.

Wing unsteady lift and moment coefficients are shown in Fig. 16. The strong gradients in the experimental results for $M_\infty = 0.82$ are associated with separated flow, which falls outside the scope of the theories investigated. Expectedly, in the subsonic case there is little difference between subsonic and Q-3-D transonic theory. The differences become larger as the Mach number increases and the flow becomes more strongly transonic. Although the Q-3-D method gives a more accurate prediction of C_Z'' and, in a qualitative sense, of C_M', the agreement with experimental results is not yet satisfactory. For a more accurate prediction, accounting for viscous effects and also for a more accurate modeling of the unsteady inviscid flow seems necessary.

Conclusions

A wing model (the LANN wing) has been fabricated and a rather complete set of transonic flow experimental data, with wide ranges of variation in Mach number, mean angle of attack, amplitude, and frequency in pitch-oscillation, has been obtained. Besides attached flow, some separated flow conditions have been included in the data set. These data are meant to support the development of computational methods for transonic unsteady viscous flow about wings.

Three numerical methods were compared with measured data. They were the XTRAN3S unsteady wing code, a version of Bailey-Ballhaus steady wing code coupled with the McNally plane boundary-layer code, and, finally, a quasi-three-dimensional method for transonic unsteady airloads computations.

The numerical results obtained with XTRAN3S and B-B/M codes have shown promise in predicting the flow over wings with shock waves, but all are far from perfect. A good match of shock location over the wing span is still not consistently attainable with either code. The small disturbance codes used in this correlation underpredicted the leading edge suction peak. The inclusion of the weakly coupled boundary layer in the inviscid wing code tended to improve its overall agreement with measured results.

The wing lift force correlated surprisingly well between the calculated and measured results, even though the pressure distributions on the wing did not match as well. The correlation of the wing moments was not as good compared to the lift correlation. This probably was caused by the fact that shock location over the wing was not correctly predicted by the theoretical methods used, especially the Bailey-Ballhaus/McNally and XTRAN3S codes.

The XTRAN3S code and the relatively low cost Q-3-D method predict qualitatively similar effects of shock waves on the unsteady airloads. Quantitative differences between both methods are probably due to inaccuracy of the prediction of the mean steady state by the XTRAN3S code, and by the approximate nature of the subsonic three-dimensional effects modeled in the Q-3-D method. The agreement with experimental results is not yet satisfactory, although in some respects improvement can be observed as compared to results of subsonic theory. Besides the approximate nature of the inviscid flow computations, the neglect of viscous effects also partly explains the disagreement between experimental and theoretical unsteady airloads.

Acknowledgments

This investigation is a cooperative program of Lockheed-Georgia Company (Gelac), Air Force Flight Dynamics Laboratory (AFWAL), NASA Langley, and the National Aerospace Laboratory (NLR). This study was supported in part by the Air Force Wright Aeronautical Laboratories, the U. S. Air Force System Command (Contract F33615-80-C-3212 and Grant AFOSR-80-0136). The Air Force technical monitor was Mr. L. J. Huttsell. Fabrication and static measurements of the model were performed under a Lockheed-Georgia Independent Research and Development project. Computing facilities were provided by NASA

Langley. The authors wish to acknowledge the following persons who have contributed to this international cooperative program: Mr. J. A. Blackwell of Lockheed-Georgia, Dr. J. J. Olsen of the U. S. Air Force, Dr. E. C. Yates of NASA Langley, and Dr. H. Tijdeman of NLR. Without their efforts, this project would not have materialized. The authors also thank Mr. L. J. Huttsell, Mr. S. Pollock, Mr. W. A. Sotomayer, Mr. D. E. Cooley of the Air Force, Mr. R. J. Zwaan, Mr. R. G. den Boer, Mr. A. N. Kraan of the NLR, Dr. J. W. Edwards, Dr. R. M. Bennett and Mr. D. A. Seidel of NASA Langley, and Mr. H. B. Little, Mr. C. M. Jenness, Mr. M. R. Myers, Mr. W. G. Grosser, Mr. R. E. Jones of the Lockheed-Georgia Company, for their support and contributions.

References

[1] Bland, S. R., "AGARD Three-Dimensional Aeroelastic Configurations," AGARD-AR-167, March 1982.

[2] Horsten, J. J., den Boer, R. G., and Zwaan, R. J., "Unsteady Transonic Pressure Measurements on a Semi-Span Wind-Tunnel Model of a Transport-Type Supercritical Wing (LANN Model)," NLR TR 82069 U, Part I and II, July 1982.

[3] Malone, J. B. and Ruo, S. Y., "LANN Wing Test Program: Aquisition and Application of Unsteady Transonic Data for Evaluation of Three-Dimensional Computer Methods," AFWAL-TR-83-3006, Feb. 1983.

[4] Steiginga, A. and Houwink, R., "Correlation of Experimental and Quasi-3-D Theoretical Unsteady Airloads on the Oscillating LANN Supercritical Wing Model," NLR TR 83003 U, 1983.

[5] Hinson, B. L. and Burdges, K. P., "Acquisition and Application of Transonic Wing and Far-field Test Data for Three-Dimensional Computational Method Evaluation," AFOSR-TR-80-0421, 1980.

[6] Tijdeman, H., "Investigations of the Transonic Flow Around Oscillating Airfoils," NLR TR 77090 U, 1977.

[7] Horsten, J. J., "Recent Developments in the Unsteady Pressure Measuring Technique at NLR," NLR MP 81055 U, 1981.

[8] Borland, C., Rizetta, D., and Yoshihara, H., "Numerical Solution of Three-Dimensional Unsteady Transonic Flow Over Swept Wings," AIAA Paper 80-1369, Snowmass, Colo., July 1980.

[9] Ballhaus, W. F., and Bailey, F. R., "Numerical Calculation of Transonic Flow About Swept Wings," AIAA Paper 72-677, Boston, Mass., June 1971.

[10] McNally, W. D., "FORTRAN Program for Calculating Compressible Laminar and Turbulent Boundary Layers in Arbitrary Pressure Gradients," NASA TN D-5681, May 1970.

[11] Steiginga, A. and Meijer, J. J., "A Revised Quasi-3-Dimensional Concept to Determine Unsteady Airloads on Oscillating High-Aspect Ratio Wings in Transonic Flow," NLR TR 82062 L, June 1982.

[12] Houwink, R., Kraan, A. N., and Zwaan, R. J., "Wind-Tunnel Study of the Flutter Characteristics of a Supercritical Wing," *Journal of Aircraft*, Vol. 19, May 1982, pp. 400-405.

[13] Houwink, R. and van der Vooren, J., "Improved Version of LTRAN2 for Unsteady Transonic Flow Computations," *AIAA Journal*, Vol. 18, Aug. 1980, pp. 1008-1010.

[14] Houwink, R., "Unsteady Viscous Transonic Flow Computations Using the LTRAN2-NLR Code Coupled with Green's Lag-Entrainment Method," Paper presented at the 2nd Symposium on Numerical and Physical Aspects of Aerodynamic Flows, California State University, Long Beach, Calif., Jan. 1983.